ELSEVIER
SAUNDERS

Neurosurg Clin N Am 16 (2005) 185–200

NEUROSURGERY
CLINICS
OF NORTH AMERICA

1.5 T: intraoperative imaging beyond standard anatomic imaging

Christopher Nimsky, MD*, Oliver Ganslandt, MD, Rudolf Fahlbusch, MD

Department of Neurosurgery, University Erlangen-Nuremberg, Schwabachanlage 6 91054 Erlangen, Germany

In contrast to the subjective estimation of the surgeon about the extent of surgery, intraoperative imaging provides an objective evaluation of surgical effects, thus acting as a measure of quality control during surgery [1]. Because of limited imaging quality, the first attempts in applying ultrasound and CT during neurosurgical procedures in the 1980s were frustrating. Since then, MRI has become the method of choice for the preoperative diagnosis of brain tumors and epilepsy. The closed-bore design and the strong fringe fields of the first MRI scanners prevented their use in the operating room, however. With the development of open MRI systems in the mid-1990s, the concept of intraoperative imaging experienced a renaissance [2–4]. The first designs were based on low-field magnets with magnetic field strengths up to 0.5 T. The use of MRI scanners in the operating environment is safe and reliable as well as applicable to neurosurgical procedures, even if these procedures have to be adapted to the MRI environment to a certain extent. In the meantime, reports on intraoperative MRI for large numbers of patients have been published [5–10].

In contrast to the development of an MRI scanner dedicated to the operating room as pioneered by Black, Jolesz, and General Electric Medical Systems (Milwaukee, Wisconsin) at the Brigham and Women's Hospital in Boston [4], we adapted, in cooperation with the Department of Neurosurgery of the University of Heidelberg and Siemens Medical Solutions (Erlangen, Germany), a low-field MRI scanner for surgical use (0.2-T Magnetom Open) [2,3]. In addition to intraoperative imaging, an integral part of our concept is the possibility of applying neuronavigation simultaneously. We prefer microscope-based neuronavigation, where the extent and localization of a tumor are superimposed on the microscope field of view through contours. Aside from standard neuronavigation based on anatomic information only, which has become a routine tool in many neurosurgical departments, we integrate preoperative functional data from magnetoencephalography (MEG) and functional MRI (fMRI) defining localizations of eloquent brain areas, such as the motor and speech areas, in individual patients, resulting in so-called "functional neuronavigation" [11–15]. Between March 1996 and July 2001, we performed intraoperative low-field MRI in 330 patients [10]. Among these procedures were 240 craniotomies, 59 transsphenoidal approaches, and 31 burr hole procedures. The simultaneous use of intraoperative MRI and functional neuronavigation allowed preservation of neurologic function despite extended resections. The most important indications for intraoperative imaging include gliomas [7–9,16,17], hormonally inactive pituitary tumors [18–21], and pharmacoresistant epilepsy [22–25]. Intraoperative MRI also enables compensation for brain shift by means of an update of the navigation system with intraoperative image data [26–29].

The diagnostic quality of intraoperative low-field MRI systems cannot compete with the image quality of routine neuroradiologic diagnosis,

This work is supported by the Deutsche Forschungsgemeinschaft and the Wilhelm-Sander-Stiftung.

* Corresponding author.
E-mail address: nimsky@nch.imed.uni-erlangen.de (C. Nimsky).

doi:10.1016/j.nec.2004.07.001

Fig. 1. (*A*) Intraoperative scene in transsphenoidal surgery. (*B–D*) For scanning, the table is rotated 160° and the patient is moved into the center of the scanner.

which is generally performed with high-field magnets. Advances in scanner design, including those resulting from active magnetic shielding, have made it possible to adapt modern high-field scanners to the surgical environment. So far, two different high-field concepts have been realized [30,31]. Basically, as in the intraoperative low-field magnet concepts, there are two possibilities: taking a standard diagnostic scanner and adapting it to the operating environment, as was done in Minneapolis with a Philips scanner (Best, The Netherlands) [31,32], or designing a high-field scanner specifically dedicated for the requirements of an operating room, as was implemented in Calgary with a ceiling-mounted magnet that is moved into the appropriate imaging position during surgery [30,33]. Our approach to realize intraoperative high-field MRI scanning combined with microscope-based neuronavigation resembles the Minneapolis setup, necessitating some kind of intraoperative patient transport for intraoperative imaging. The active magnetic shielding of the high-field magnet results in the 5-G zone being relatively close to the scanner such that the adaptation of a rotating operating table enables combining intraoperative high-field MRI with microscope-based neuronavigation [34]. The main operating position where navigation can be applied is located in the fringe field of the scanner; use of all standard neurosurgical equipment is possible there. In this way, our concept of intraoperative MRI with integration of microscope-based neuronavigation in the low magnetic fringe field [35] can now be applied for high-field magnets. Our operating room was appropriately reconstructed between August 2001 and March 2002. We have been able to operate on patients using intraoperative high-field MRI and integrated microscope-based neuronavigation since the end of April 2002.

Operating room setup

Intraoperative high-field MRI

A rotating surgical table (Trumpf, Saalfeld, Germany) is adapted to a 1.5-T Magnetom Sonata Maestro Class scanner (Siemens Medical Solutions), which is placed in an operating room with radiofrequency (RF) shielding (Figs. 1, 2). The scanner consists of a superconductive 1.5-T magnet with a length of 160 cm and an inner bore diameter of 60 cm equipped with a gradient system with an effective field strength of up to

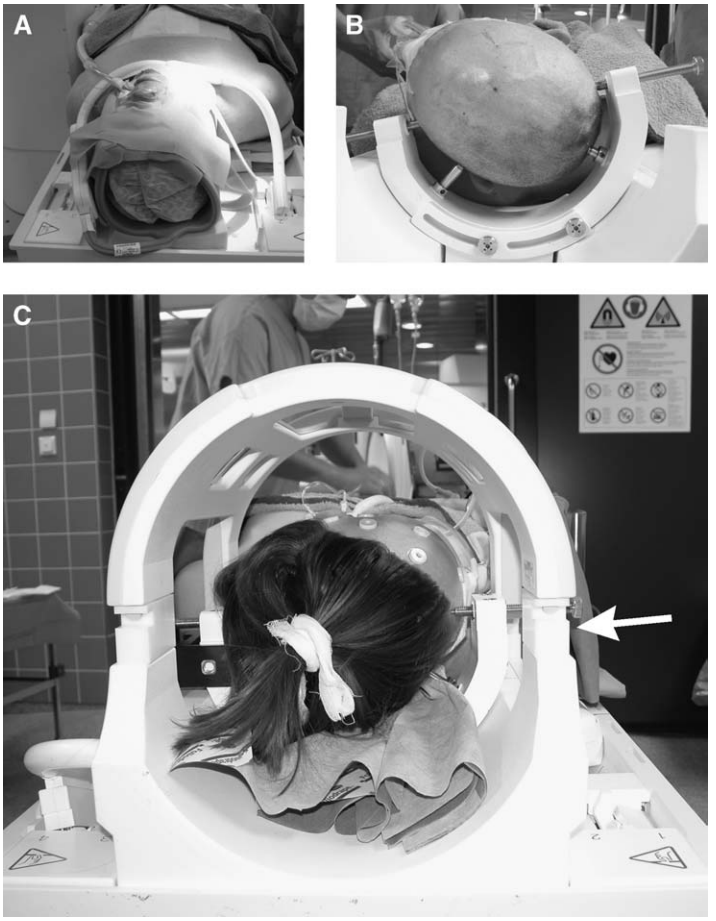

Fig. 2. Different possibilities of coil placement. (*A*) In transsphenoidal surgery, a flexible coil is attached to the head and surgical access is not impeded. (*B*) In craniotomy procedures, the head is fixed in an MRI-compatible head holder, which is placed in the lower part of the standard head coil. (*C*) Sterile adapters (*white arrow*) are placed on the lower part of the head coil, allowing sterile placement of the upper part of the head coil during surgery (image depicts situation before surgery to show the details without draping).

69 mT/m and an effective slew rate of up to 346 T/m/s. The rotating surgical table can be locked into various positions. The principal surgical position is at 160°, with the patient's head at the 5-G line (4-m distance to the center of the scanner). The height of the table, the angle of tilt, and the lateral tilt can be remotely controlled. For imaging, the table is rotated manually for safety reasons so that the table is turned into the axis of the scanner (see Fig. 1).

The ceiling outlet for laminar airflow (Luwa, Frankfurt, Germany) is located above the main operating position. The laminar airflow output is surrounded by a band of fluorescent lamps for optimal illumination. For scanning, the illumination can be turned off from the control room. The entire operating theater has MRI-compatible spot-room lighting. Two ceiling-mounted surgical lamps (Heraeus Med, Hanau, Germany) are installed at the main surgical position. Movable MRI-compatible surgical lamps (Heraeus Med) can be used at the second surgical position in the high magnetic field at the dorsal opening of the scanner. MRI-compatible ventilation (Servo 900C; Siemens Medical Solutions) and MRI-compatible monitoring (Invivo Research, Orlando, Florida) are available for anesthesia. Vital parameters are transferred outside the RF cabin by wireless 2.4-GHz data transfer. The perfusors and infusion pumps are shielded for MRI compatibility (MRI-Caddy; MIPM, Mammendorf, Germany) [36]. All standard gas lines are available on service outlets

Table 1
Sequences used in intraoperative high-field MRI

Sequence	Slice thickness (mm)	TR (ms)	TE (ms)	FOV (mm)	In-plane resolution (mm)	No. acquisitions	Total scan time
Localizer	10	20	50	280	1.1 × 1.1	1	9 s
Pituitary tumors							
T2-HASTE	5	1000	89	230	0.89 × 0.89	5	25 s
T1-SE	3	450	12	270	0.52 × 0.87	4	4 min 57 s
T2-TSE	3	3850	111	210	0.41 × 0.58	4	7 min 17 s
Gliomas/epilepsy surgery							
T2-TSE	4	6490	98	230	0.44 × 0.74	3	5 min 39 s
FLAIR	4	10,000	103	230	0.44 × 0.74	1	6 min 2 s
T1-SE	4	525	17	230	0.89 × 0.89	2	3 min 59 s
EPI	5	30,000	85	230	1.79 × 1.79	2	3 min
MPRAGE	1	2020	4.38	250	0.49 × 0.49i	1	8 min 39 s
Metabolic and functional imaging							
MRS-CSI	10	1600	135	160	6.7 × 6.7	2	12 min 45 s
fMRI	3	1580	60	192	3 × 3	1	3 min 13
DTI	1.9	9200	86	240	1.87 × 1.87	5	5 min 31 s

Abbreviations: CSI, chemical shift imaging; DTI, diffusion tensor imaging; EPI, echo planar imaging; FLAIR, fluid-attenuated inversion recovery; FOV, field of view; HASTE, half-Fourier single-shot turbo spin echo; i, interpolated; min, minutes; MPRAGE, magnetization prepared rapid acquisition gradient echo sequence; MRS, magnetic resonance spectroscopy; s, seconds; SE, spin echo; TE, echo time; TR, repetition time; TSE, turbo spin echo.

at different places in the RF cabin. Compressed air is integrated to operate drills. The service outlets include sockets connected to different electrical circuits so that selected sockets can be switched off from a switchboard in the MRI control room to prevent artifacts generated by individual devices.

The NC4 Multivision microscope (Zeiss, Oberkochen, Germany) is installed at the left side of the head outside the 5-G line. The microscope and other potentially interfering devices are automatically switched off for the MRI measurements. The microscope videotape is documented using Medimage software (Vepro, Pfungstadt, Germany) and in parallel as a recording on commercial S-VHS tapes. Both systems are installed in the MRI control room. Two flat-monitor screens (17.4 in, AS4431ID; Iyamo, Nagano-Shi, Japan) mounted on a ceiling arm (Ondal, Hünfeld, Germany) display the microscope image, the image from the MRI console, or various personal computer (PC) applications. There is also a wall-mounted PC console using Autoview200 (Avocent, Munich, Germany), with which the various PC systems, such as the videotape documentation and the navigation system, can be operated from inside the RF cabin. There is an identical console in the MRI control room. A mobile in-room MRI console is available in the RF room for operating the scanner. The 5-G and 200-G lines are marked on the floor. The 200-G line is also marked by a raised stainless steel strip as a mechanical threshold. All equipment not completely MRI-compatible, such as the navigation microscope and the height-adjustable surgeon's chair, are mechanically secured to the wall of the RF room. The instrument table and the various rotating stools are fully MRI-compatible (Trumpf).

An MRI-compatible four-point head holder made of fiberglass-reinforced plastic was used for head fixation during the craniotomy and burr hole procedures. It is integrated into the common system circular polarized head coil (see Fig. 2B) [37]. The upper part of the head coil may be sterilized using plasma sterilization. Sterile adapters placed onto the lower part of the head coil ensure the possibility of sterile draping (see Fig. 2C). In transsphenoidal surgery that does not require head fixation, imaging is performed using a U-shaped flexible coil adapted to the head (see Fig. 2A). After the patient is moved into the center of the scanner, certain circuits are switched off, including the fluorescent lamps, the operating microscope, and the part of the navigation system that is located in the RF cabin. Imaging then starts with a localizer sequence (all sequence parameters are listed in Table 1).

In transsphenoidal surgery, T2-weighted half-Fourier single-shot turbo spin echo (HASTE) sequences in coronal and sagittal orientations

are measured next to give a quick overview. HASTE imaging allows one to obtain a rough estimation of the extent of the resection, allowing nearly immediate continuation of surgery if a tumor remnant is depicted. Afterward, T1-weighted coronal and sagittal spin echo sequences are applied. Additionally, high-resolution, T2-weighted, turbo spin echo sequences are measured. The protocol in transsphenoidal pituitary surgery was modified after having acquired increased experience. Measuring of the T1-weighted images was abandoned, because T2-weighted imaging provided sufficient and even more reliable information than the T1-weighted images, especially regarding better delineation of the intrasellar and parasellar structures.

In glioma surgery, the imaging protocol includes the following axial sequences: T2-weighted turbo spin echo, fluid-attenuated inversion recovery (FLAIR), T1-weighted spin echo, and echo planar imaging dark fluid. In case the tumor showed contrast enhancement in the preoperative images, the T1-weighted axial spin echo sequence was repeated after intravenous application of gadolinium-diethylenetriamine pentaacetic acid at a rate of 0.2-mL/kg of body weight. Afterward, the 1.0-mm, isotropic, three-dimensional (3-D) magnetization prepared rapid acquisition gradient echo sequence (MPRAGE) data set, which is used for navigation, was measured, allowing free-slice reformatting and intraoperative updating of the navigation system [27,28]. In epilepsy surgery and other applications (eg, biopsies), a reduced scanning protocol was applied. If intraoperative imaging resulted in further tumor removal, imaging was repeated after completion of the resection before wound closure. Contrast medium was not applied repeatedly. If preoperative scanning was performed after head fixation and anesthesia induction, identical sequence parameters were used so that the identical pre- and intraoperative slices could be displayed side by side, facilitating image interpretation greatly.

Neuronavigation

Neuronavigation support is provided by the VectorVision Sky Navigation System (BrainLab, Heimstetten, Germany). A fiberoptic connection ensures MRI-compatible integration into the RF room. The camera used to monitor the positions of the microscope and other instruments is ceiling mounted, as is the touch screen that is used to operate the navigation system. A 1.0-mm, isotropic, 3-D MPRAGE data set was acquired before surgery as a navigational reference data set in which functional data could be integrated. For registration, five adhesive skin fiducials were placed in a scattered pattern on the head surface before imaging and registered with a pointer after their position was defined in the 3-D data set, or a LASER scanning device (z-touch; BrainLab) [38] was used for referencing. Functional data from MEG and fMRI, which were acquired before surgery, were integrated into the 3-D data set [11–15]. Furthermore, data from diffusion tensor imaging (DTI) depicting the course of major white matter tracts were integrated, and metabolic maps from magnetic resonance spectroscopy (chemical shift imaging [CSI]) were coregistered to the navigation data set in selected cases [39]. Repeated landmark checks were performed to ensure overall ongoing clinical application accuracy. In case intraoperative imaging depicted some remaining tumor that should be removed, intraoperative image data were used for updating the navigation system. After a rigid registration of pre- and intraoperative images (ImageFusion software; BrainLAB), all data were transferred to the navigation computer, and the initial patient registration file was then restored such that no repeated patient registration procedure was needed.

Clinical experience

Three hundred thirteen patients have been examined with intraoperative high-field MRI through the end of February 2004. Among these operations were 118 transsphenoidal procedures, 47 burr hole procedures, and 148 craniotomies (Table 2). The major groups were patients with gliomas and pituitary adenomas. Intraoperative high-field MRI is a safe and reliable procedure, we did not encounter any adverse events as a result of the high magnetic field, and there were no ferromagnetic accidents as a result of the use of standard instruments in the fringe field at the 5-G zone. With respect to intraoperative work flow, we found a distinct improvement over our previous designs [2,10,35]. The time necessary for intraoperative imaging has been greatly reduced. In general, it took less than 2 minutes from the time the neurosurgeon decided to use intraoperative imaging until the imaging was actually started. With all the anesthesia lines to and from the patient passing through the surgical table's center of rotation, there were no delays, because

Table 2
Histopathologic findings and types of procedures in 313 patients investigated with intraoperative high-field MRI

Histopathologic finding	cr	ts	bh	Total
Pituitary adenoma	3	95	—	98
Glioma	75	—	22	97
Gliosis/hippocampal sclerosis (epilepsy surgery)	29	—	—	29
Craniopharyngioma	4	13	—	17
Meningioma	9	—	—	9
Lymphoma	4	—	5	9
Cavernoma	9	—	—	9
Dysembryoplastic neuroepithelial tumor	5	—	—	5
Gliomatosis	2	—	2	4
Rathke cleft cyst	—	4	—	4
Metastasis	2	—	1	3
Chordoma	—	2	—	2
Others	6	4	3	13
No histology obtained:				
Craniopharyngioma cyst puncture	—	—	9	9
Other cystic lesions	—	—	5	5
Total	148	118	47	313

Abbreviations: bh, burr hole procedure; cr, craniotomy; ts, transsphenoidal surgery.

no rearrangement of the anesthesia equipment was necessary. Also, the preoperative handling, including patient positioning and navigation registration, was less time-consuming. We expect that the possibility of automatic registration of images, which is under development, will result not only in further time saving but in further improved accuracy during clinical applications.

Intraoperative imaging was technically possible in all cases. We encountered technical difficulties in only one case. In one of the first transsphenoidal procedures, a coil cable broke during use of the flexible coil such that the coil had to be replaced. No major artifacts related to the operating room environment were observed. The ability to turn off the fluorescent lamps and specific power outlets from the MRI control room proved helpful. We did not encounter increased problems with artifacts because of the high-field setup but rather fewer artifacts than with the previous system. This may be mainly a result of the improved operating room design, including better flexibility to eliminate artifacts from devices located in the operating room itself as well as an improved coil design for intraoperative imaging, which was one of the major problems with the initial low-field setup.

The flexibility of the rotating surgical MRI table during surgery is similar to that of a standard surgical table. The head holder integrated into the head coil allows some variability of access; the patient can be placed in the supine and prone position or the head can be turned up to a horizontal position. Full lateral placement of the whole patient is only possible in young patients because of the inner core size of the scanner (60 cm). Access to the craniotomy site is limited to a certain extent. The coil adapters sometimes handicapped access to the craniotomy site. A new head holder with a dedicated eight-channel MRI coil is just being developed. We expect that this new device will improve the ergonomics for the neurosurgeon without decreasing image quality.

The intraoperative image quality obtained is clearly superior to that of our previous intraoperative low-field (0.2-T) system. Even the comparison of pre- and intraoperative images did not indicate any significant limitation. Fig. 3 gives an impression of the enhanced image quality of the intraoperative high-field system in comparison to our previous low-field system in two similar cases of frontal low-grade gliomas. We think that the clearly improved image quality will result in more reliable information regarding the extent of resection (ie, presence of residual tumor tissue and its exact location). Aside from improved image quality, the high-field scanner allows significantly shorter examination times such that a more detailed sequence protocol can be measured within the same time frame.

In 92 (29.4%) of all 313 patients, intraoperative MRI resulted in a modification of the surgical strategy (ie, an extension of the resection or a correction of the placement of a biopsy needle or a catheter). Concerning the major application of intraoperative imaging, which is resection control in pituitary adenomas and gliomas, these numbers are even higher (30 [40%] of 74 patients and 31 [43%] of 72 patients, respectively). Comparing these rates with our previous low-field experience (34% and 26%, respectively) [21,40] supports the impression that the clearly improved image quality of the high-field system may also result in increased rates of extended resections.

Transsphenoidal pituitary surgery

Among the 95 patients with pituitary adenomas who were operated on via the transsphenoidal approach, 74 had an intra- and suprasellar extension that seemed accessible and removable

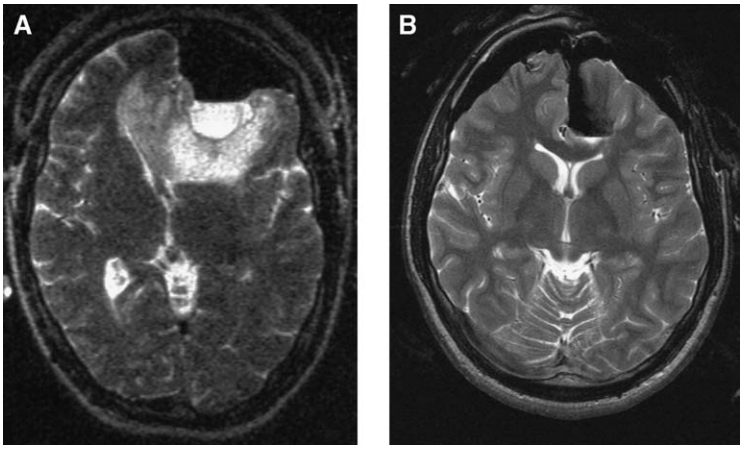

Fig. 3. Comparison of intraoperative image quality in similar clinical cases of left frontal low-grade gliomas examined with T2-weighted imaging. (*A*) Low-field MRI with a 0.2-T Magnetom Open scanner (Siemens Medical Solutions, Erlangen, Germany). (*B*) High-field MRI with a 1.5-T Magentom Sonata scanner.

by the transsphenoidal approach. Repeated inspection of the surgical field during intraoperative MRI revealed some remaining tumor that could be at least partially removed in 30 patients. In 20 of these patients, the resection could be completed, resulting in an increase in the rate of complete removal from 56.7% (42 of 74 patients) to 83.8% (62 of 74 patients). Reliable imaging of suprasellar tumor removal was possible in all cases. Fig. 4 illustrates a typical example of a pituitary adenoma with a distinct suprasellar extension, which could be removed completely. In contrast to the low-field systems, where evaluation of the intrasellar space was rarely possible [21], even the structures of the cavernous sinus could now be evaluated reliably in most patients. Ultra-early (ie, intraoperative) visualization of tumor remnants that are not removable allows the immediate planning of further postoperative treatment options, such as surveillance, radiation therapy, or transcranial surgery. Otherwise, further planning would only be possible some 2 to 3 months after surgery because of early postoperative imaging artifacts preventing reliable image evaluation after transsphenoidal surgery [21,41].

Transsphenoidal surgery of craniopharyngiomas could also be monitored reliably by intraoperative imaging. High-resolution T2-weighted imaging provided valuable information about the extent of resection (Fig. 5). Despite the clearly improved image quality of high-field MRI compared with low-field MRI with regard to craniopharyngioma removal, it is too early to decide whether high-field MRI is more sensitive in the detecting small tumor islets that may give rise to craniopharyngioma recurrence compared with low-field MRI [42].

Burr hole procedures

Exclusion of intracerebral hemorrhage and confirmation of the biopsy site were the major aspects of intraoperative imaging in burr hole procedures (n = 47). In nine patients with large cystic craniopharyngiomas, the cyst could be punctured with a catheter guided by navigation. In four of these patients, intraoperative MRI revealed that the catheter had not penetrated the cyst wall such that no drainage of the cyst to the lateral ventricle was established, leading to a repeated puncture, which was then successful as proved by repeated intraoperative imaging. In five further patients, cysts originating from other tumors could be punctured without any problems. In all 33 burr hole biopsies, a histologic diagnosis could be obtained. Side-by-side display of corresponding pre- and intraoperative slices enabled direct evaluation of the biopsy site (Fig. 6). During the time of intraoperative imaging, frozen section analysis of parts of the biopsy sample was also performed to confirm that a pathologic specimen was obtained. In three patients, intraoperative imaging resulted in a correction of the biopsy needle path. In one patient who was operated on directly in the high magnetic field, the advancement of the biopsy needle could be

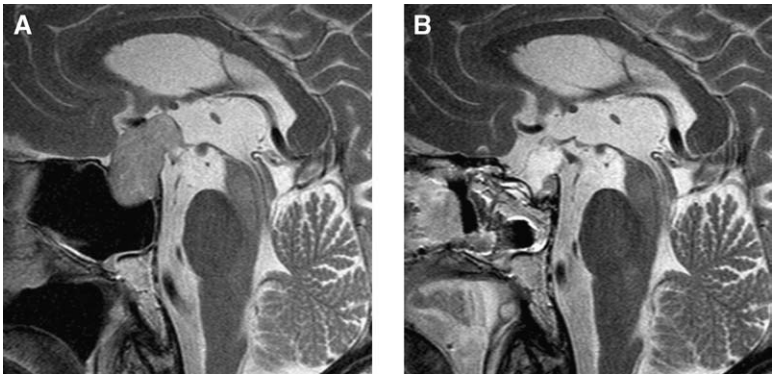

Fig. 4. (*A*) Preoperative T2-weighted imaging in a 53-year-old man with a pituitary adenoma with a distinct suprasellar extension. (*B*) Intraoperative imaging confirms complete removal.

monitored by scanning with a true fast imaging with steady-state precession sequence with a single-slice scan duration of 190 milliseconds.

Glioma surgery

Regarding the treatment of gliomas, at present, the standard treatment is maximum safe resection and, for high-grade gliomas, subsequent adjuvant treatment, such as radio- and chemotherapy [43–45]. With respect to patients undergoing glioma resection (n = 72), intraoperative imaging revealed complete tumor removal initially in 18 (25%) patients. Extension of the resection because of intraoperative imaging resulted in a final gross total removal of 40.3% of gliomas. Of the 29 patients with a finally completed resection, 11 (37.9%) resections were attributable to further tumor removal after intraoperative MRI. In 23 patients with incomplete tumor removal, further resection was abandoned because of the infiltration of eloquent brain cortex or critical anatomic structures despite obvious residual tumor on intraoperative imaging. Additional resection in 31 (43.1%) patients as the result of intraoperative MRI significantly reduced the percentage of final tumor volume compared with first intraoperative MRI. According to a volumetric assessment, the percentages of residual tumor volume were significantly decreased from the first intraoperative scan to the final scan [46]. Even in the subgroup of patients in which no complete resection was intended because of infiltration of eloquent brain areas, intraoperative MRI led to further tumor reduction in 46.5% (20 of 43) of the patients, reducing the tumor volume significantly. In low-grade gliomas, there is little question that complete removal of all tumor tissue is an ideal treatment that may lead to cure. If residual tumor is left

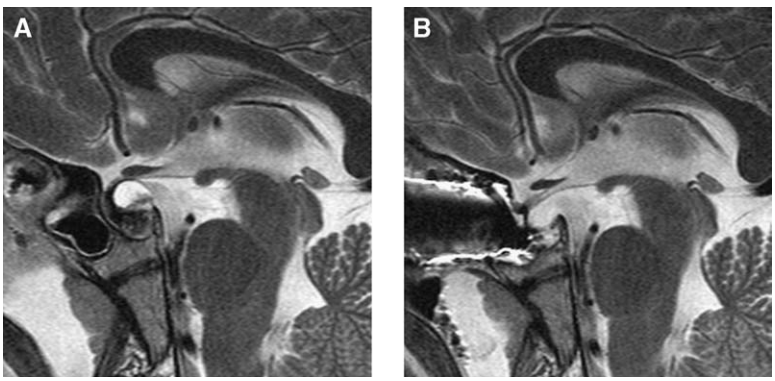

Fig. 5. (*A*) T2-weighted imaging in a 10-year-old girl with a craniopharyngioma that could be removed completely via a transsphenoidal approach. (*B*) Note the high imaging quality with the clear delineation of the pituitary stalk and the infundibulum in the intraoperative images.

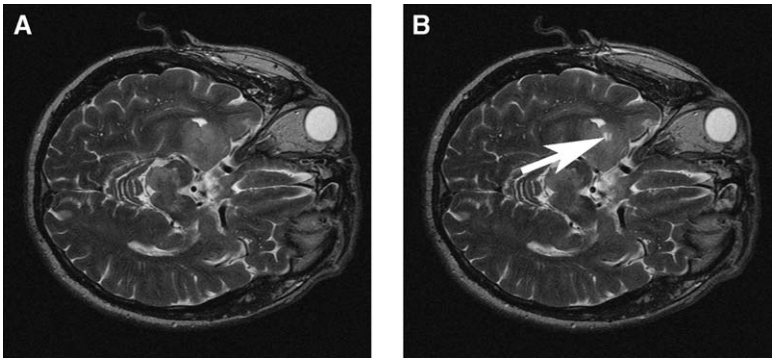

Fig. 6. (*A*) Intraoperative imaging in a biopsy procedure of a diffuse glioma (extending into the internal capsule and into the brain stem) in a 59-year-old man. (*B*) Intraoperative imaging confirms the preplanned navigated biopsy site in the right temporal lobe (*white arrow*). Frozen section analysis confirmed a high-grade glioma, and histologic examination revealed a diffuse astrocytoma, World Health Organization grade III.

behind, it eventually degenerates into a glioblastoma multiforme, limiting the life expectancy of the patient [1]. Even in high-grade gliomas, several reports have supported the benefit of aggressive tumor removal, which was associated with longer survival of patients [47–50]. Fig. 7 depicts an example of resection control in a high-grade glioma. As in transsphenoidal surgery, T2-weighted imaging proved to be most helpful. FLAIR imaging often showed diffuse enhancement at the resection border. Side-by-side and overlay display of corresponding pre- and intraoperative images facilitated imaging interpretation, especially to distinguish between surgically induced changes and tumor remnants.

Other procedures

In all patients, intraoperative MRI provided immediate intraoperative quality control not only in respect to the extent of a resection or the positioning of a catheter or a biopsy needle but with regard to complication avoidance, because we did not encounter any rebleeding. Another interesting indication for intraoperative MRI is epilepsy surgery [22–25]. In epilepsy surgery for nonlesional temporal lobe epilepsy, intraoperative MRI allowed clear delineation of the extent of tailored temporal lobectomies. Furthermore, localization of subdural and hippocampal strip electrodes could be defined by intraoperative imaging.

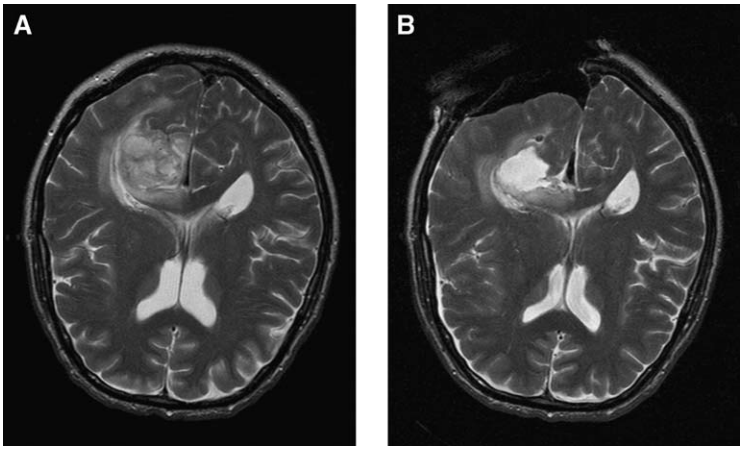

Fig. 7. Right occipital World Health Organization grade IV glioblastoma in a 67-year-old man. T2-weighted imaging reveals complete removal of the main tumor mass and depicts the remaining infiltration zone in the posterior corpus callosum (*A*, preoperative image; *B*, intraoperative image).

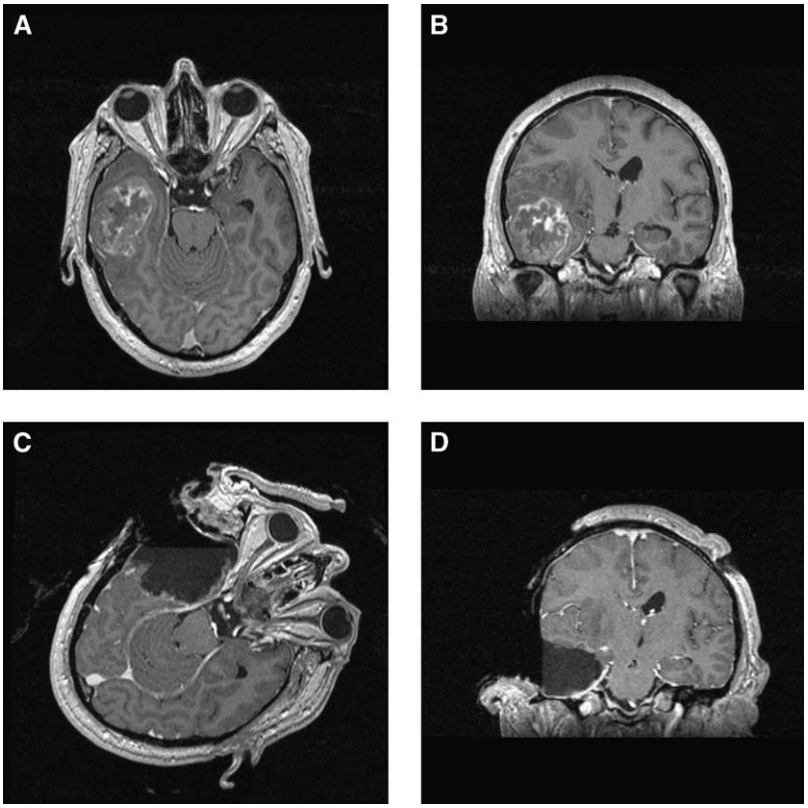

Fig. 8. T1-weighted magnetization prepared rapid acquisition gradient echo sequence images of a right temporal World Health Organization grade IV glioblastoma in a 57-year-old man. Intraoperative imaging confirms the removal of the contrast-enhancing tumor parts (*A, B*: preoperative images; *C, D*: intraoperative images; *A, C*: corresponding axial slices; *B, D*: corresponding coronal slices).

Anatomic neuronavigation guidance

The various other tumor entities that were investigated by intraoperative MRI in smaller numbers included mainly tumors with a difficult location, where navigation guidance was essential, and intraoperative imaging was used to identify tumor remnants and localize them by intraoperative updating of the neuronavigation system, thus compensating for brain shift. The integrated microscope-based neuronavigation was used without problems and with good clinical accuracy. Navigation accuracy was not impeded by the magnetic fringe field. The mean registration error ranged from 0.3 to 2.9 mm. In all navigation cases, the localization error of an additional fiducial, which was not used for the registration, allowed us to document a low target registration error. Only in two cases did the navigation setup fail because of software problems. In total, navigation was applied in 170 patients. The navigation was updated in 42 patients (24.7% of the patients in which navigation was applied) without difficulty. This led to reliable identification of the residual tumor parts and compensated for brain shift. Compared with previous setups that necessitated intraoperative patient reregistration [26–29], which was time-consuming, the implemented update procedure that restores the initial patient registration data facilitated updating. Excluding the patients operated on by a transsphenoidal approach, in which navigation was applied in selected cases only (n = 6), navigation was administered in 84% (164 of 195) of all patients, demonstrating the close integration of imaging and navigation. The remaining 16% of patients who did not undergo navigation were mainly patients with pharmacoresistant epilepsy undergoing tailored temporal lobe resection. In these patients, navigation was not applied routinely, because the various intraoperative anatomic

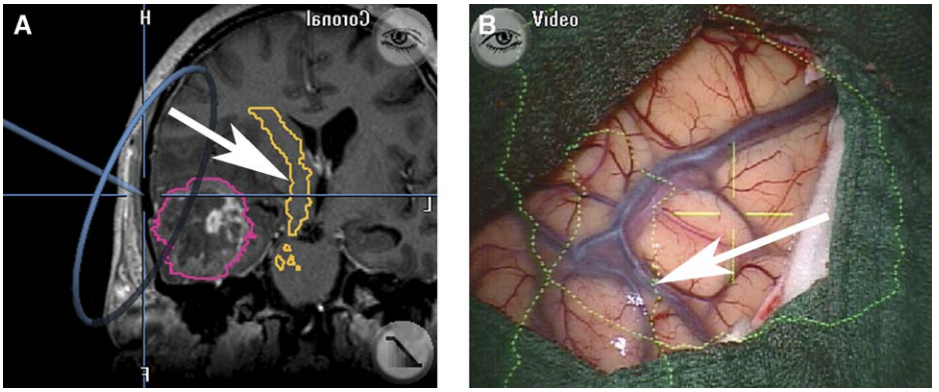

Fig. 9. Navigation screen of the same patient as in Fig. 8. (*A*) The displaced right pyramidal tract is visualized by diffusion tensor imaging and integrated into the navigational data set (*arrow*, coronal T1-weighted image of navigation screen). (*B*) Corresponding microscope view just after dural opening; the tumor contour as well as the contour of the right pyramidal tract is displayed (*arrow*).

landmarks of the temporal lobe were sufficient for reliable guidance. Scanning the 3-D data set, which is used for patient registration, just before surgery after induction of anesthesia and head fixation excluded shifting of registration markers and was a prerequisite for low registration error.

Functional neuronavigation and functional imaging

Functional neuronavigation (ie, integrating functional data into the anatomic navigation data sets) is an important add-on to intraoperative MRI because it prevents resections that are too extensive, which would otherwise result in new neurologic deficits. We had integrated functional or metabolic data in 65 patients and observed prolonged new postoperative neurologic deficits in only 4 of them. To date, data from MEG and fMRI are routinely integrated in functional neuronavigation, allowing identification of eloquent brain areas, such as the motor area and speech-related areas [11,14,15]. This method is open to integrate further modalities, such as magnetic resonance spectroscopy and DTI. Both methods have been used recently as new diagnostic tools in patients with gliomas [51–56]. Magnetic resonance spectroscopy data may provide further information on the diffuse tumor border. Integration of metabolic maps into the neuronavigation data sets enables spatial correlation of metabolic data and histopathologic findings [39].

Functional data from MEG and fMRI only localize function at the brain surface; however, neurologic deficits can occur during tumor resection as a result of damage to deeper structures, such as major white matter tracts. DTI can be used not only to delineate tumor borders but to display the course of white matter tracts, such as the pyramidal tract [57–61]. Knowledge of the course of major white matter tracts in relation to a tumor may help to prevent new postoperative neurologic deficits [62,63]. Registration of these data with the navigation data set [64] should facilitate the intraoperative preservation of these eloquent structures if the intraoperative changes of the brain anatomy, known as brain shift, are taken into account. Fig. 8 illustrates standard anatomic preoperative and corresponding intraoperative imaging in a right temporal glioblastoma. We had integrated DTI data depicting the displaced course of the pyramidal tract into the navigational data set so that these data could be visualized during surgery (Fig. 9). Intraoperative functional imaging (ie, applying intraoperative DTI) revealed a marked shifting of the pyramidal tract because of tumor resection (Fig. 10). As a consequence of this shifting, the preoperative functional data are no longer valid, so the neurosurgeon can no longer rely on the navigation if this shifting is not compensated for. Therefore, it is necessary not only that intraoperative anatomic data be used to compensate for the effects of brain shift [28,29,65] but that functional data be updated [66]. Mathematic models that describe the brain shift phenomenon using finite elements should be helpful in this respect [67,68]. At present, however, only intraoperative functional imaging provides reliable data on the actual intraoperative situation. Whether intraoperative

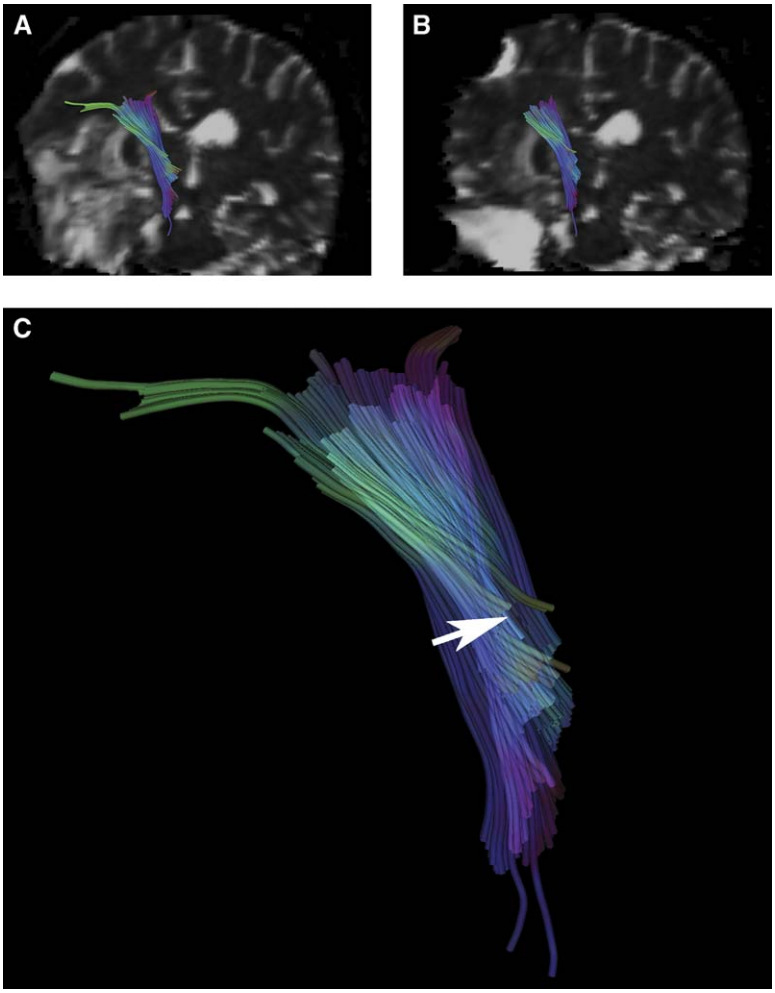

Fig. 10. Comparison between the preoperative (*A*) and intraoperative (*B*) fiber tract visualization of the pyramidal tract with the coregistered B-0 images depicts an inward shifting of the right pyramidal tract after tumor removal. (*C*) The semitransparent overlay of the pre- and intraoperative fiber tracts illustrates the inward shifting, which amounts to approximately 6 mm (*arrow*).

fMRI, despite the open skull, is reliably possible at all is under investigation. Electrical stimulation of the median and tibial nerves as a passive stimulation paradigm may allow identification of the somatosensory cortex [69]. The next steps will be the integration of DTI-based tractography data into the neuronavigation data set along with fMRI, because the combination of fMRI and DTI provides valuable information that cannot be extracted using either method alone [62,70]. Regarding the pyramidal tract, using the fMRI data as seed regions for the DTI fiber-tracking algorithms would be an elegant method.

Other further applications of intraoperative high-field MRI may take place in the field of vascular surgery. Magnetic resonance angiography shows the complete clipping of an aneurysm, and the use of diffusion-weighted imaging should also allow us to evaluate intraoperative blood supply, thus preventing reduced perfusion [71]. Furthermore, intraoperative MRI may also prove useful in spinal surgery, such as for the resection of complex intramedullary tumors or drainage of syringomyelias.

At present, intraoperative high-field MRI with integrated microscope-based neuronavigation is

certainly one of the most sophisticated technical methods providing reliable intraoperative quality control. Intraoperative high-field MRI provides intraoperative anatomic images of high quality that are up to the standard of pre- and postoperative neuroradiologic imaging. Compared with the previous low-field MRI systems that were used for intraoperative imaging, not only is the image quality clearly superior but the imaging spectrum is much wider and the intraoperative work flow is improved. Furthermore, high-field MRI offers various modalities beyond standard anatomic imaging, such as magnetic resonance spectroscopy, DTI, and fMRI.

Acknowledgments

The authors thank the entire team of physicists and computer scientists at our neurocenter for their efforts in image processing, namely, P. Grummich, P. Hastreiter, and A. Stadlbauer. They are also grateful to A.G. Sorensen (Department of Radiology/Nuclear Magnetic Resonance Center, Massachusetts General Hospital, Boston, MA) for providing the DTI processing software. Furthermore, they acknowledge the continuing assistance of E. Müller and T. Vetter (Siemens Medical Solutions, Erlangen, Germany).

References

[1] Bradley WG. Achieving gross total resection of brain tumors: intraoperative MR imaging can make a big difference. AJNR Am J Neuroradiol 2002; 23(3):348–9.

[2] Steinmeier R, Fahlbusch R, Ganslandt O, Nimsky C, Buchfelder M, Kaus M, et al. Intraoperative magnetic resonance imaging with the Magnetom open scanner: concepts, neurosurgical indications, and procedures. A preliminary report. Neurosurgery 1998;43(4):739–48.

[3] Tronnier VM, Wirtz CR, Knauth M, Lenz G, Pastyr O, Bonsanto MM, et al. Intraoperative diagnostic and interventional magnetic resonance imaging in neurosurgery. Neurosurgery 1997;40(5): 891–902.

[4] Black PM, Moriarty T, Alexander E III, Stieg P, Woodard EJ, Gleason PL, et al. Development and implementation of intraoperative magnetic resonance imaging and its neurosurgical applications. Neurosurgery 1997;41(4):831–45.

[5] Schwartz RB, Hsu L, Wong TZ, Kacher DF, Zamani AA, Black PM, et al. Intraoperative MR imaging guidance for intracranial neurosurgery: experience with the first 200 cases. Radiology 1999; 211(2):477–88.

[6] Seifert V, Zimmermann M, Trantakis C, Vitzthum HE, Kuhnel K, Raabe A, et al. Open MRI-guided neurosurgery. Acta Neurochir (Wien) 1999;141(5):455–64.

[7] Black PM, Alexander E III, Martin C, Moriarty T, Nabavi A, Wong TZ, et al. Craniotomy for tumor treatment in an intraoperative magnetic resonance imaging unit. Neurosurgery 1999;45(3):423–33.

[8] Schneider JP, Schulz T, Schmidt F, Dietrich J, Lieberenz S, Trantakis C, et al. Gross-total surgery of supratentorial low-grade gliomas under intraoperative MR guidance. AJNR Am J Neuroradiol 2001;22(1):89–98.

[9] Wirtz CR, Knauth M, Staubert A, Bonsanto MM, Sartor K, Kunze S, et al. Clinical evaluation and follow-up results for intraoperative magnetic resonance imaging in neurosurgery. Neurosurgery 2000;46(5): 1112–22.

[10] Nimsky C, Ganslandt O, Tomandl B, Buchfelder M, Fahlbusch R. Low-field magnetic resonance imaging for intraoperative use in neurosurgery: a 5 year experience. Eur Radiol 2002;12(11):2690–703.

[11] Kober H, Möller M, Nimsky C, Vieth J, Fahlbusch R, Ganslandt O. New approach to localize speech relevant brain areas and hemispheric dominance using spatially filtered magnetoencephalography. Hum Brain Mapp 2001;14(4):236–50.

[12] Kober H, Nimsky C, Möller M, Hastreiter P, Fahlbusch R, Ganslandt O. Correlation of sensorimotor activation with functional magnetic resonance imaging and magnetoencephalography in presurgical functional imaging: a spatial analysis. Neuroimage 2001;14(5):1214–28.

[13] Kober H, Nimsky C, Vieth J, Fahlbusch R, Ganslandt O. Co-registration of function and anatomy in frameless stereotaxy by contour fitting. Stereotact Funct Neurosurg 2002;79(3–4):272–83.

[14] Nimsky C, Ganslandt O, Kober H, Möller M, Ulmer S, Tomandl B, et al. Integration of functional magnetic resonance imaging supported by magnetoencephalography in functional neuronavigation. Neurosurgery 1999;44:1249–56.

[15] Ganslandt O, Fahlbusch R, Nimsky C, Kober H, Möller M, Steinmeier R, et al. Functional neuronavigation with magnetoencephalography: outcome in 50 patients with lesions around the motor cortex. J Neurosurg 1999;91:73–9.

[16] Bohinski RJ, Kokkino AK, Warnick RE, Gaskill-Shipley MF, Kormos DW, Lukin RR, et al. Glioma resection in a shared-resource magnetic resonance operating room after optimal image-guided frameless stereotactic resection. Neurosurgery 2001; 48(4):731–44.

[17] Knauth M, Wirtz CR, Tronnier VM, Aras N, Kunze S, Sartor K. Intraoperative MR imaging increases the extent of tumor resection in patients with high-grade gliomas. AJNR Am J Neuroradiol 1999; 20(9):1642–6.

[18] Martin CH, Schwartz R, Jolesz F, Black PM. Transsphenoidal resection of pituitary adenomas in an intraoperative MRI unit. Pituitary 1999;2: 155–62.
[19] Pergolizzi RS, J.,Nabavi A, Schwartz RB, Hsu L, Wong TZ, Martin C, et al. Intra-operative MR guidance during trans-sphenoidal pituitary resection: preliminary results. J Magn Reson Imaging 2001; 13(1):136–41.
[20] Bohinski RJ, Warnick RE, Gaskill-Shipley MF, Zuccarello M, van Loveren HR, Kormos DW, et al. Intraoperative magnetic resonance imaging to determine the extent of resection of pituitary macroadenomas during transsphenoidal microsurgery. Neurosurgery 2001;49(5):1133–44.
[21] Fahlbusch R, Ganslandt O, Buchfelder M, Schott W, Nimsky C. Intraoperative magnetic resonance imaging during transsphenoidal surgery. J Neurosurg 2001;95(3):381–90.
[22] Schwartz TH, Marks D, Pak J, Hill J, Mandelbaum DE, Holodny AI, et al. Standardization of amygdalohippocampectomy with intraoperative magnetic resonance imaging: preliminary experience. Epilepsia 2002;43(4):430–6.
[23] Kaibara T, Myles ST, Lee MA, Sutherland GR. Optimizing epilepsy surgery with intraoperative MR imaging. Epilepsia 2002;43(4):425–9.
[24] Buchfelder M, Fahlbusch R, Ganslandt O, Stefan H, Nimsky C. Use of intraoperative magnetic resonance imaging in tailored temporal lobe surgeries for epilepsy. Epilepsia 2002;43(8):864–73.
[25] Buchfelder M, Ganslandt O, Fahlbusch R, Nimsky C. Intraoperative magnetic resonance imaging in epilepsy surgery. J Magn Reson Imaging 2000; 12:547–55.
[26] Nabavi A, Black PM, Gering DT, Westin CF, Mehta V, Pergolizzi RS Jr, et al. Serial intraoperative magnetic resonance imaging of brain shift. Neurosurgery 2001;48(4):787–98.
[27] Nimsky C, Ganslandt O, Cerny S, Hastreiter P, Greiner G, Fahlbusch R. Quantification of, visualization of, and compensation for brain shift using intraoperative magnetic resonance imaging. Neurosurgery 2000;47(5):1070–80.
[28] Nimsky C, Ganslandt O, Hastreiter P, Fahlbusch R. Intraoperative compensation for brain shift. Surg Neurol 2001;56(6):357–64.
[29] Wirtz CR, Bonsanto MM, Knauth M, Tronnier VM, Albert FK, Staubert A, et al. Intraoperative magnetic resonance imaging to update interactive navigation in neurosurgery: method and preliminary experience. Comput Aided Surg 1997; 2:172–9.
[30] Sutherland GR, Kaibara T, Louw D, Hoult DI, Tomanek B, Saunders J. A mobile high-field magnetic resonance system for neurosurgery. J Neurosurg 1999;91(5):804–13.
[31] Hall WA, Liu H, Martin AJ, Pozza CH, Maxwell RE, Truwit CL. Safety, efficacy, and functionality of high-field strength interventional magnetic resonance imaging for neurosurgery. Neurosurgery 2000;46(3):632–42.
[32] Hall WA, Martin AJ, Liu H, Nussbaum ES, Maxwell RE, Truwit CL. Brain biopsy using high-field strength interventional magnetic resonance imaging. Neurosurgery 1999;44(4):807–14.
[33] Kaibara T, Saunders JK, Sutherland GR. Advances in mobile intraoperative magnetic resonance imaging. Neurosurgery 2000;47(1):131–8.
[34] Nimsky C, Ganslandt O, Keller VB, Fahlbusch R. Preliminary experience in glioma surgery with intraoperative high-field MRI. Acta Neurochir Suppl (Wien) 2003;88:21–9.
[35] Nimsky C, Ganslandt O, Kober H, Buchfelder M, Fahlbusch R. Intraoperative magnetic resonance imaging combined with neuronavigation: a new concept. Neurosurgery 2001;48(5):1082–91.
[36] Schmitz B, Nimsky C, Wendel G, Wienerl J, Ganslandt O, Jacobi K, et al. Anesthesia during high-field intraoperative magnetic resonance imaging—experience with 80 consecutive cases. J Neurosurg Anesthesiol 2003;15(3):255–62.
[37] Nimsky C, Ganslandt O, Fischer H, Oppelt A, Vetter T, Distler P, et al. Kombination aus Kopffixation und Kopfspule für neurochirurgische Operationen. Siemens Technik Report 2000;3(6):64–5.
[38] Raabe A, Krishnan R, Wolff R, Hermann E, Zimmermann M, Seifert V. Laser surface scanning for patient registration in intracranial image-guided surgery. Neurosurgery 2002;50(4):797–803.
[39] Ganslandt O, Stadlbauer A, Nimsky C, Buslei R, Blümcke I, Moser E, et al. Integration of MR spectroscopy into neuronavigation for stereotactic definition of tumor infiltration zone. In: Lemke H, Vannier M, Inamura K, Farman A, Doi K, Reiber J, editors. CARS 2003, vol. ICS 1256. Amsterdam: Elsevier; 2003. p. 1339.
[40] Nimsky C, Ganslandt O, Buchfelder M, Fahlbusch R. Glioma surgery evaluated by intraoperative low-field magnetic resonance imaging. Acta Neurochir Suppl (Wien) 2003;85:55–63.
[41] Dina TS, Feaster SH, Laws ER, Davis DO. MR of the pituitary gland postsurgery: serial MR studies following transsphenoidal resection. AJNR Am J Neuroradiol 1993;14:763–9.
[42] Nimsky C, Ganslandt O, Hofmann B, Fahlbusch R. Limited benefit of intraoperative low-field magnetic resonance imaging in craniopharyngioma surgery. Neurosurgery 2003;53(1):72–81.
[43] Gupta T, Sarin R. Poor-prognosis high-grade gliomas: evolving an evidence-based standard of care. Lancet Oncol 2002;3(9):557–64.
[44] Laws E. Surgical management of intracranial gliomas—does radical resection improve outcome? Acta Neurochir Suppl (Wien) 2003;85(85):47–53.
[45] Nicolato A, Gerosa MA, Fina P, Iuzzolino P, Giorgiutti F, Bricolo A. Prognostic factors in low-grade supratentorial astrocytomas: a uni-multivari-

ate statistical analysis in 76 surgically treated adult patients. Surg Neurol 1995;44(3):208–23.
[46] Nimsky C, Ganslandt O, Keller VB, Romstöck J, Fahlbusch R. Intraoperative high-field magnetic resonance imaging: implementation and experience with the first 200 patients. Radiology, in press.
[47] Albert FK, Forsting M, Sartor K, Adams HP, Kunze S. Early postoperative magnetic resonance imaging after resection of malignant glioma: objective evaluation of residual tumor and its influence on regrowth and prognosis. Neurosurgery 1994; 34(1):45–61.
[48] Chandler KL, Prados MD, Malec M, Wilson CB. Long-term survival in patients with glioblastoma multiforme. Neurosurgery 1993;32(5):716–20.
[49] Lacroix M, Abi-Said D, Fourney DR, Gokaslan ZL, Shi W, DeMonte F, et al. A multivariate analysis of 416 patients with glioblastoma multiforme: prognosis, extent of resection, and survival. J Neurosurg 2001;95(2):190–8.
[50] Obwegeser A, Ortler M, Seiwald M, Ulmer H, Kostron H. Therapy of glioblastoma multiforme: a cumulative experience of 10 years. Acta Neurochir (Wien) 1995;137(1–2):29–33.
[51] Tzika AA, Cheng LL, Goumnerova L, Madsen JR, Zurakowski D, Astrakas LG, et al. Biochemical characterization of pediatric brain tumors by using in vivo and ex vivo magnetic resonance spectroscopy. J Neurosurg 2002;96(6):1023–31.
[52] Rock J, Hearshen D, Scarpace L, Croteau D, Gutierrez J, Fisher J, et al. Correlations between magnetic resonance spectroscopy and image-guided histopathology, with special attention to radiation necrosis. Neurosurgery 2002;51(4):912–20.
[53] Law M, Cha S, Knopp E, Johnson G, Arnett J, Litt A. High-grade gliomas and solitary metastases: differentiation by using perfusion and proton spectroscopic MR imaging. Radiology 2002;222(3): 715–21.
[54] Hall WA, Martin A, Liu H, Truwit CL. Improving diagnostic yield in brain biopsy: coupling spectroscopic targeting with real-time needle placement. J Magn Reson Imaging 2001;13(1):12–5.
[55] Dowling C, Bollen AW, Noworolski SM, McDermott MW, Barbaro NM, Day MR, et al. Preoperative proton MR spectroscopic imaging of brain tumors: correlation with histopathologic analysis of resection specimens. AJNR Am J Neuroradiol 2001;22(4):604–12.
[56] Beppu T, Inoue T, Shibata Y, Kurose A, Arai H, Ogasawara K, et al. Measurement of fractional nisotropy using diffusion tensor MRI in supratentorial astrocytic tumors. J Neurooncol 2003;63: 19–116.
[57] Kamada K, Houkin K, Takeuchi F, Ishii N, Ikeda J, Sawamura Y, et al. Visualization of the eloquent motor system by integration of MEG, functional, and anisotropic diffusion-weighted MRI in functional neuronavigation. Surg Neurol 2003;59(5):352–62.
[58] Tummala RP, Chu RM, Liu H, Truwit CL, Hall WA. Application of diffusion tensor imaging to magnetic-resonance-guided brain tumor resection. Pediatr Neurosurg 2003;39:39–43.
[59] Westin CF, Maier SE, Mamata H, Nabavi A, Jolesz F, Kikinis R. Processing and visualization for diffusion tensor MRI. Med Image Anal 2002;6: 93–108.
[60] Witwer BP, Moftakhar R, Hasan KM, Deshmukh P, Haughton V, Field A, et al. Diffusion-tensor imaging of white matter tracts in patients with cerebral neoplasm. J Neurosurg 2002;97(3): 568–75.
[61] Yamada K, Kizu O, Mori S, Ito H, Nakamura H, Yuen S, et al. Brain fiber tracking with clinically feasible diffusion-tensor MR imaging. Initial experience Radiology 2003;227(1):295–301.
[62] Hendler T, Pianka P, Sigal M, Kafri M, Ben-Bashat D, Constantini S, et al. Delineating gray and white matter involvement in brain lesions: three-dimensional alignment of functional magnetic resonance and diffusion-tensor imaging. J Neurosurg 2003;99(6):1018–27.
[63] Clark CA, Barrick TR, Murphy MM, Bell BA. White matter fiber tracking in patients with space-occupying lesions of the brain: a new technique for neurosurgical planning? Neuroimage 2003;20(3): 1601–8.
[64] Coenen VA, Krings T, Mayfrank L, Polin RS, Reinges MH, Thron A, et al. Three-dimensional visualization of the pyramidal tract in a neuronavigation system during brain tumor surgery: first experiences and technical note. Neurosurgery 2001; 49(1):86–93.
[65] Hastreiter P, Engel K, Soza G, Bauer M, Wolf M, Ganslandt O, et al. Remote analysis for brain shift compensation. In: Niessen W, Viergever M, editors. Medical image computing and computer assisted intervention (MICCAI). Berlin: Springer; 2001. p. 1248–9.
[66] Wolf M, Vogel T, Weierich P, Niemann H, Nimsky C. Automatic transfer of preoperative fMRI markers into intraoperative MR-images for updating functional neuronavigation. Institute of Electronics, Information and Communication Engineers Transactions Information and Systems 2001; E84-D(12):1698–704.
[67] Miga MI, Paulsen KD, Hoopes PJ, Kennedy FE, Hartov A, Roberts DW. In vivo modeling of interstitial pressure in the brain under surgical load using finite elements. J Biomech Eng 2000;122(4): 354–63.
[68] Ferrant M, Warfield SK, Nabavi A, Jolesz F, Kikinis R. Registration of 3D intraoperative MR images of the brain using a finite element biomechanical model. In: Delp SL, DiGioia AM, Jaramaz B, editors. Medical image computing and computer-assisted intervention (MICCAI). Berlin: Springer; 2000. p. 19–28.

[69] Gasser TG, Sandalcioglu EI, Wiedemayer H, Hans V, Gizewski E, Forsting M, et al. A novel passive functional MRI paradigm for preoperative identification of the somatosensory cortex. Neurosurg Rev 2004;27(2):106–12.

[70] Guye M, Parker GJ, Symms M, Boulby P, Wheeler-Kingshott CA, Salek-Haddadi A, et al. Combined functional MRI and tractography to demonstrate the connectivity of the human primary motor cortex in vivo. Neuroimage 2003;19(4): 1349–60.

[71] Sutherland GR, Kaibara T, Wallace C, Tomanek B, Richter M. Intraoperative assessment of aneurysm clipping using magnetic resonance angiography and diffusion-weighted imaging. Technical case report Neurosurgery 2002;50(4):893–8.